Improved High-Resolution SNAILS DTI with A Spiral-in Navigator

C. Liu[1], R. Bammer[1], M. Moseley[1]

[1]Stanford University, Stanford, CA, United States

INTRODUCTION: Variable density (VD) spiral has been applied in SNAILS (Self-Navigated InterLeaved Spiral) for the acquisition of high-resolution diffusion weighted images (1, 2). It has been shown that by oversampling the center of **k**-space, SNAILS provides the capability to correct for the motion-induced phase errors. Furthermore, the increased image SNR resulting from oversampling improves the tolerance for residual motion-induced phase errors. On the other hand, excessive oversampling of the center **k**-space increases readout time, which may increase off-resonance blurring and noise correlation. Here, a method is proposed to improve SNAILS by using a short spiral-in navigator to acquire the phase map. This extra navigator reduces the oversampling factor of the VD spiral and hence improves the acquisition efficiency, while maintaining a moderate oversampling and hence redundancy to compensate residual phase errors. *In vivo* high-resolution diffusion tensor imaging (DTI) are demonstrated with this improved SNAILS.

METHOD: In SNAILS, the oversampled center **k**-space data provide a low resolution phase map which can be used to correct for motion-induced phase error prior to combining all interleaf data. Furthermore, the phase navigation combined with the conjugate gradient based phase correction method has enabled SENSE SNAILS and has been successfully used to acquire high-resolution multi-shot diffusion-weighted images (3).

For both phase correction and parallel imaging of SNAILS, an accurate phase map is important for high quality DTI. In this work, to improve the phase navigation, a short spiral-in navigator is acquired prior to the formation of the spin echo. Following the navigator, an accelerated VD spiral is implemented for image acquisition after the spin echo. Specifically, the spiral-in navigator is designed as a single-interleaf conventional spiral (4) that fully samples a 32x32 Cartesian grid. The navigator data are only used for navigation purpose and are not added to the final reconstructed images. This implementation offers users the flexibility to specify the resolution of the spiral-in and the spiral-out images independently on the scanner in real time.

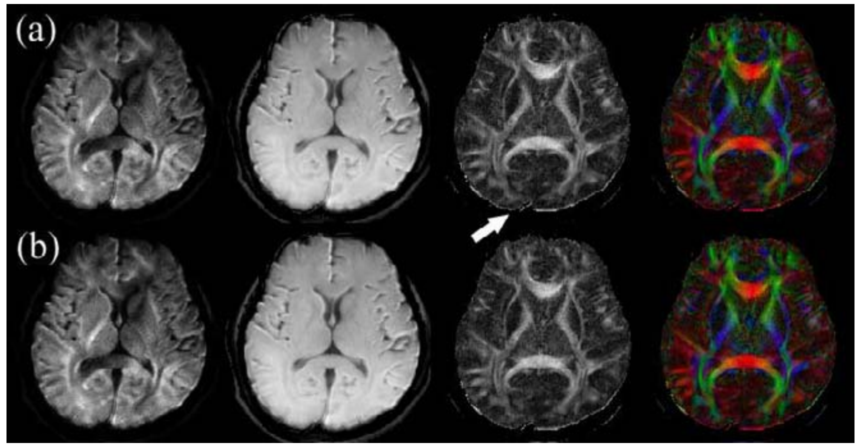

Figure 1. High resolution SNAILS DTI ($\alpha = 4$) reconstructed (a) with spiral-in navigator; (b) without navigator. Images from left to right are: diffusion-weighted image, isotropic-weighted image, FA map and color-coded FA map.

In vivo diffusion measurements were performed on healthy volunteers with an 8-channel header coil (MR Devices) on a GE SIGNA 1.5T scanner. The following parameters were used: TR/TE = 2.5s/56ms, G_{max} = 50mT/m, b = 800s/mm^2, FOV = 24cm, acquisition matrix size = 256x256, BW = ±125 kHz, and 20 interleaves. No cardiac gating was used. Six diffusion gradient directions [(1 1 0), (1 0 1), (0 1 -1), (-1 1 0), (0 1 1), (1 0 -1)] were applied to acquire the diffusion tensor. The total scan time was 11.6 minutes for 2 NEX. The scan was repeated for two VD spiral pitch factors: $\alpha = 4$ and 2, with larger α meaning more oversampling at the center **k**-space. For comparison, images were reconstructed both with and without the spiral-in navigator.

RESULTS: Figures 1 and 2 compare a set of a typical diffusion-weighted image, an isotropic-weighted image and the corresponding fractional anisotropy (FA) maps. In Figure 1, $\alpha = 4$, and Figure 2, $\alpha = 2$. In both figures, row (a) shows results obtained with the spiral-in navigator; row (b) shows results without the navigator, in which the center VD spiral data provide phase and sensitivity estimation. Both figures illustrate that the spiral-in navigator improves the image contrast and SNR, especially for smaller pitch factors (Figure 2). The improvement is most obvious in the FA maps (Figure 2a and b). Additionally, by reducing α thus reducing the amount of oversampling, both the diffusion-weighted images and the FA maps appears much sharper. The improvement is obvious, for example, in the posterior end of sagittal striatum (arrows in Figures 1 and 2).

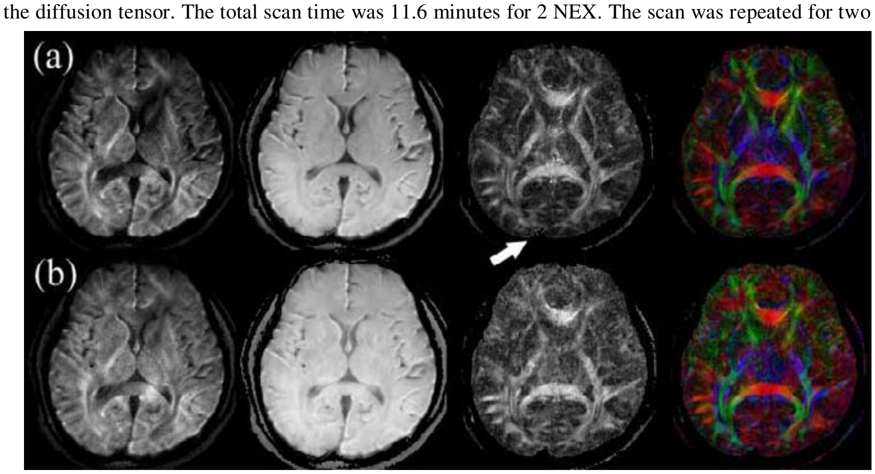

Figure 2. High resolution SNAILS DTI ($\alpha = 2$) reconstructed (a) with spiral-in navigator; (b) without spiral-in navigator. With the navigator, images have better contrast and SNR.

DISCUSSION: We have demonstrated that a short spiral-in navigator can significantly improve the quality of high-resolution SNAILS DTI. The spiral-in navigator provides more reliable phase navigation than the center **k**-space data alone, which results in higher SNR. The improvement is most significant for smaller pitch factors. Furthermore, the spiral-in navigator reduces the necessity to excessively oversample the center **k**-space. Because of this oversampling, the readout time for each interleaf of the VD spiral is typically longer for larger pitch factors. For example, with the parameters given in this abstract, each interleaf of a VD spiral has around 4486 sampling points for $\alpha = 4$, and 3512 sampling points for $\alpha = 2$. The spiral-in navigator enables a smaller pitch factor, which results in sharper images. On the other hand, with the readout time kept the same, the navigator can shorten the scan time of SNAILS by using a smaller pitch factor and less interleaves. Additionally, the spiral-in image can be used to co-register different interleaves.

It is important to realize that there is a tradeoff between SNR and image sharpness when the number of interleaves is fixed. Although the spiral-in navigator can provide a good estimation of the phase maps, *in vivo* residual errors may persist. Therefore, it is important to keep an oversampling factor in the VD spiral to compensate any residual artifacts. In conclusion, by carefully selecting the pitch factor, SNAILS in combination with an extra navigator can be optimized to achieve high quality and high resolution DTI.

ACKNOWLEDGMENTS: NIH-1R01NS35959, NIH-1R01EB002771, Lucas Foundation, Center of Advanced MR Technology of Stanford (NCRR P41 RR 09784)

REFERENCES: 1) Liu C, et al. Magn Reson Med 2004; 52:1388-1396. 2) D.H. Kim, et al. Magn Reson Med. 2003, 50: 214-219. 3) Liu C, et al. Proc ISMRM. 2005, p10.